PHYSICAL REVIEW B **66**, 161201(R) (2002)

Diffuse x-ray scattering study of interfacial structure of self-assembled conjugated polymers

Jun Wang,[1,*] Y. J. Park,[2] K.-B. Lee,[3] H. Hong,[4] and D. Davidov[4]
[1]*Beijing Synchrotron Radiation Facility, Institute of High Energy Physics, Chinese Academy of Sciences, P.O. Box 918(2-7), Beijing 100039, People's Republic of China*
[2]*Pohang Accelerator Laboratory, Pohang University of Science and Technology, Pohang 790-784, Korea*
[3]*Department of Physics, Pohang University of Science and Technology, Pohang 790-784, Korea*
[4]*Racah Institute of Physics, The Hebrew University of Jerusalem, Jerusalem 91904, Israel*
(Received 25 June 2002; published 9 October 2002)

The interfacial structures of self-assembled heterostructures through alternate deposition of conjugated and nonconjugated polymers were studied by x-ray reflectivity and nonspecular scattering. We found that the interfacial width including the effects of both interdiffusion and interfacial roughness (correlated) was mainly contributed by the latter one. The self-assembled deposition induced very small interdiffusion between layers. The lateral correlation length $\xi_{\parallel}$ grew as a function of deposition time (or film thickness) described by a power law $\xi_{\parallel} \propto t^{\beta/H}$ and was also observed from the off-specular scattering.

DOI: 10.1103/PhysRevB.66.161201 PACS number(s): 61.10.−i, 68.35.Ct, 68.55.−a

Organic multilayered structures are actively being developed for next-generation optoelectronic devices.[1–3] The self-assembled heterostructures through alternate deposition of conjugated and nonconjugated polymers, which have different dielectric constants and band gaps, could be regarded as multiquantum wells, and the quantum size effects were also observed.[3–5] One of the most important factors that affect the device performance is the nature of the interfaces of the multilayers.[6] Nevertheless, there have been few reports in the literature on the interfacial structure of the self-assembled modulated heterostructures containing deuterated conjugated polymers, especially on the lateral structure information of the rough interface, which is important for interface morphology.

X-ray specular reflectivity and nonspecular diffuse scattering have been widely used to characterize interfacial structures in a nondestructive manner.[6–17] While x-ray specular reflectivity yields averaged information in the direction perpendicular to the surface of the film, nonspecular diffuse scattering is sensitive to the lateral structure of rough interfaces. The lateral information of an interface leads to structural details about the morphology of interfaces of a layer system, and can be obtained by the analysis of the diffuse scattering intensity caused by lateral inhomogeneities.[7–17] In this paper, we report x-ray specular reflectivity and nonspecular diffuse scattering measurements from self-assembled modulated heterostructures of conjugated and nonconjugated polymers. Based on the x-ray results, the interfacial morphology of the polymer-based heterostructure is described, which includes not only the average information perpendicular to the surface of the film, but also the lateral structure information of the interfaces.

The sample in our experiment was prepared by the method of layer-by-layer self-assembly of oppositely charged polyelectrolytes on a glass substrate.[6] The heterostructure consists of two types of polyelectrolytes, one is a precursor of the conjugated polymer, deuterated poly(phenylenevinylene) (D-PPV), and the other is a nonconjugated polymer, the polycation poly(allylamine hydrochloride) (PAH) at the polyanion poly(styrene-4-sulfonate) (SPS). For improving the adhesion of the film and positively charging the substrate, a thin film of poly(ethylene-imine) (PEI) was deposited on a float glass substrate. The modulated structure can be described as substrate/PEI/$([\mathrm{SPS/PAH}]_3[\mathrm{SPS/(Eu\text{-}PPV)}])_m$, where m is the repetition number of bilayers. Europium (Eu) was added into the D-PPV layer to improve its electro-optical property. The detail description about the fabrication process was presented in Ref. 6.

X-ray specular reflectivity and nonspecular scattering measurements were carried out using synchrotron radiation at a bending magnet beam line 3C2 of the Pohang Light Source with a Huber four-circle diffractometer. The x ray was monochromated by a Si(111) double crystal monochrometer, the photon energy was selected at the L_{III} absorption edge 6.977 keV of Eu.

The Paratt formalism[18,19] was used to analyze the x-ray reflectivity data from the sample $([\mathrm{SPS/PAH}]_3[\mathrm{SPS/(Eu\text{-}PPV)}])_m$, with $m=21$. Since the electron density of SPS is very similar to that of PAH, we divided the repeating unit $[\mathrm{SPS/PAH}]_3[\mathrm{SPS/(Eu\text{-}PPV)}]$ into two parts as the $(\mathrm{SPS/PAH})_3\mathrm{SPS}$ layer (space layer) with thickness d_s and the (Eu-PPV) layer (active layer) with thickness d_A. The refractive index n_j in the jth layer is $n_j = 1-\delta_j - i\beta_j$, δ_j and β_j are related to dispersion and absorption, j denotes the numbering of interfaces starting at the surface of the heterostructure. The Fresnel reflection coefficient for a smooth interface is

$$r_{j,j+1} = \frac{n_j \sin\theta_j - n_{j+1}\sin\theta_{j+1}}{n_j \sin\theta_j + n_{j+1}\sin\theta_{j+1}},$$

where θ_j is the incident angle of the jth layer. The amplitude ratio of the jth layer,

$$R_j = \frac{r_{j,j+1} + R_{j+1}e^{-2ik_{j+1}d_{j+1}}}{1 + r_{j,j+1}R_{j+1}e^{-2ik_{j+1}d_{j+1}}},$$

$d_j = d_{Aj} + d_{Sj}$ is the repeat unit thickness, $k_j = (2\pi/\lambda)n_j \sin\theta_j$ is the vertical component of the wave vector in the jth layer. The reflected intensity $I = |R_0|^2$. For a

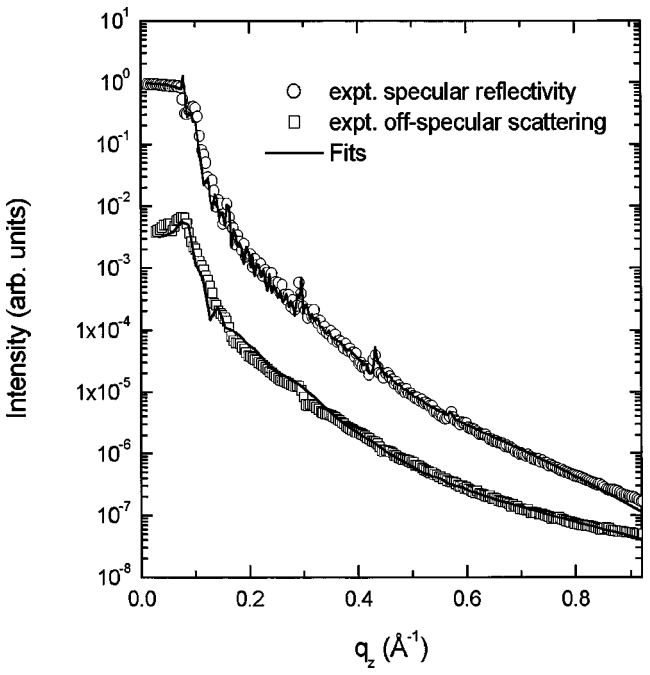

FIG. 1. True specular reflectivity and off-specular diffuse scattering with offset angle $\Delta\theta_i = 0.05°$. Solid lines are the fits to the reflectivity represented by circles based on the Parratt formalism and the off-specular scattering intensity represented by squares based on DWBA theory.

rough interface, the interface roughness was incorporated into the calculation as a factor of $\exp(-2k_j k_{j+1}\sigma_j)$ multiplied to the Fresnel coefficient of the jth layer.[20] σ_j is the interfacial width of the jth layer.

The x-ray specular reflectivity measurement from the sample is shown in Fig. 1 as open circles, while the solid line was the fitting result, which reproduced the experimental curve very well. The x-ray reflectivity data shown here was corrected for geometrical effects (footprint correction). The off-specular scattering intensity, shown in Fig. 1 as squares, was subtracted from the raw specular reflection data to separate the specular intensity from the diffuse one. The fitting parameters include the repeat unit thickness d, the ratio of thickness of d_A/d, the total interfacial width σ, and the dispersion of the space layer δ_s and the active layer δ_A.

Compared with the thicknesses of the space and active layers, the value of the interfacial width σ indicates that the active layer can be separated by the space layer, that is to say, the excitons or electron-hole pair could be confined in the active layer. The interfacial width obtained from the specular reflectivity includes the effects of both interfacial roughness and interdiffusion, which can be expressed as $\sigma_t^2 = \sigma_c^2 + \sigma_d^2$, where σ_c and σ_d represent the correlated roughness and interdiffusion.[21] This will be discussed later. The existence of the Bragg reflections up to the third order demonstrates that the modulated structure has a good periodicity; it also shows that the layer-by-layer self-assembly technique is potentially a practical way for preparing the polymer-based heterostructure for light-emitting diodes. The reflectivity is sensitive to the electron-density profile of the film in the vertical direction. The weak specular intensities at Bragg peaks indicate the small contrast of the electron density of the two parts in the repeat unit. It is consistent with the fit result shown in Table I.

TABLE I. Parameters obtained from simultaneous fits of the specular reflectivity and nonspecular diffuse scattering.

Repeat unit thickness d (Å)	140.5
Space layer thickness d_s (Å)	112.4
Active layer thickness d_A (Å)	28.1
Dispersion of the space layer δ_s	5.9×10^{-6}
Dispersion of the active layer δ_A	6.5×10^{-6}
Total interfacial roughness σ (Å)	14
Substrate roughness σ_s (Å)	6
Maximum lateral correlation length $\xi_\parallel$ (Å)	2400
Minimum lateral correlation length $\xi_\parallel$ (Å)	500
Maximum correlated interface roughness σ_c (Å)	13
Minimum correlated interface roughness σ_c (Å)	6
Vertical correlation length $\xi_\perp$ (Å)	400
Roughness exponent (Hurst parameter) H	0.4

Specular scans perpendicular to the interfaces do not provide the lateral interfacial information. It is also difficult to separate out σ_c and σ_d from specular reflectivity alone. For investigating the lateral interface structure, two types of scans, the offset $\theta/2\theta$ scan, which probes in both q_z and q_x directions for the off-specular scattering, and the transverse scan along q_x direction, were conducted. The description of the experimental setup has been published elsewhere.[22]

Sinha *et al.*[23] developed a theoretical method for analysis of nonspecular scattering from a single rough surface by using the distorted-wave Born approximation (DWBA). The extension to the layered system within DWBA has been worked out by Holy and co-workers[21,24] and others.[15] The formula for calculating the diffuse scattering intensity in DWBA can be expressed as

$$\left(\frac{d\sigma}{d\Omega}\right)_{\text{diff}} = \frac{k_0^4}{16\pi^2}\sum_{i,j=1}^{N}(n_i^2 - n_{i+1}^2)(n_j^2 - n_{j+1}^2)^* \times \sum_{m,n=0}^{3} S\,\frac{D_m^{i+1}D_n^{j+1*}}{q_{mz}^{i+1}q_{nz}^{j+1*}}\, e^{-1/2[\sigma_i^2(q_{mz}^{i+1})^2 + \sigma_j^2(q_{nz}^{j+1*})^2]} \times \int d^2X[\exp(q_{mz}^{i+1}q_{nz}^{j+1*}C_{ij}(X) - 1]\exp(iq_xX). \quad (1)$$

Here $C(X)$ is the so-called height-height correlation function. For an isotropic solid surface, for a self-affine surface $C(X)$ has the form[23] $C(X) = \sigma_c^2\exp(-X/\xi_\parallel)^{2H}$, where $0 < H < 1$ is referred to as the roughness exponent to describe how jagged the surface is, $\xi_\parallel$ is the lateral correlation length of the interface, which represents a characteristic horizontal cutoff when a self-affine interface saturates at large length scales, σ_c is the correlated interface roughness, which denotes the part of the total interfacial width replicated from the lower interface to the upper layer, X is the lateral coordinate of interface atomic positions. It shows that the lateral roughness

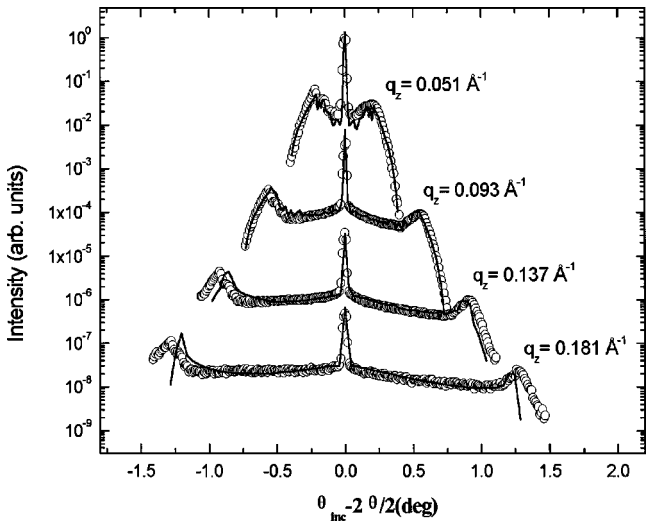

FIG. 2. Rocking curves in the region $0.051 \leqslant q_z \leqslant 0.181$. The circles are the experimental data and the solid lines are the fitting result. For clarity, curves were vertically shifted.

structure of the interface is expressed only by the correlation function in the differential cross section of the diffuse scattering. The cross correlation function between the ith and jth interfaces, $C_{ij}(X)$, can be expressed[15,24,25] as $C_{ij}(X) = \sigma_{c,i}\sigma_{c,j} \exp(-X/\xi_{\|})^{2H} \exp(-|z_i - z_j|/\xi_{\perp})$, $\xi_{\perp}$ represents the vertical correlation length along the layer growth direction, which was assumed to be constant in our analysis. The detailed definition of all parameters appearing in Eq. (1) can be found in Refs. 15, 21, 24, and 25.

The off-specular scattering intensity with an offset angle of 0.05° from the sample is shown in Fig. 1, and the measured rocking curves at the multilayer Bragg peaks in the region $0.051 \leqslant q_z \leqslant 0.181$ are shown in Fig. 2. The ''Yoneda wings'' [26] are observed in the series of rocking curves at a different order of Bragg peaks when the incidence angle or the exit angle is equal to the critical angle of the total reflection of the film. The symbol represents the experimental intensity while the solid lines are calculation results. Equation (1) was used to calculate the diffuse scattering intensities. We found that the usual assumption of a single average value for the lateral correlation length $\xi_{\|}$ and the correlated roughness σ_c for all interfaces in the simulation process was not suitable for our sample.

It is worth noting that the dynamical scaling behavior exhibited in the evolution of the interface morphology of a thin film during deposition can be extracted from our experiment. The interfacial width σ and the lateral correlation length $\xi_{\|}$ are described by two dynamic scaling laws[15,27,28] $\sigma \propto t^{\beta}$, and $\xi_{\|} \propto t^{\beta/H}$, where t is the deposition time, which is assumed to be directly proportional to the film thickness. We assume that the lateral correlation length increases from the value $\xi_{\|,\min}$ at the interface of the buffer as $\xi_{\|,j} = [\xi_{\|}^2 + C^2(j^{\beta/H})^2]^{1/2}$, j denotes the number of the jth interface. Here we assume that the lateral correlation length of the interface of A/B is the same as that of the interface of B/A. C is given by $\xi_{\|,\max} = Ct^{\beta/H}$. We used the lateral correlation length of the top interface $\xi_{\|,\max}$ and that of the buffer interface $\xi_{\|,\min}$ as fitting parameters. Therefore, $\xi_{\|,j} = (\xi_{\|,\min}^2 + [(N-j)/N]^{2\beta/H}(\xi_{\|,\max}^2 - \xi_{\|,\min}^2))^{1/2}$. Using this approach, we conclude that the in-plane correlation length increases with growth time, based on the value at each interface. Furthermore, the roughness exponent H obtained from the diffuse scattering analysis is 0.4, which is close to the value for the Kardar-Parisi-Zhang model of surface growth.[29] Compared to other previous studies, it is smaller than the value given by Ref. 30, where we studied plasma polymer films at different deposition rates, and the value for Mo films sputter deposited onto silicon studied by us.[31] That means the thin-film dynamical growth is quite complicated for different material systems or with different surface diffusion mechanisms.

In our simulation analysis, if we set the σ_c as an average value for all interfaces, the fitting can not reproduce the diffuse scattering curves well. If the substrate roughness σ_s from specular reflectivity was increased from 6 to 14 Å, we could make fitting results look good. But this is not correct; $\sigma_s = 6$ Å, which is obtained from the specular reflectivity analysis, is accurate, based on the Parrat formalism. We believe that the reason for this discrepancy is the following. It is commonly known that for metal multilayers, σ_s is small, usually about 2–3 Å, close to its substrate material roughness, and the total roughness σ_{tot} is about several angstroms. However, for our polymer multilayers, σ_{tot} is as big as 14 Å, the interdiffusion width σ_d is pretty small. In other words, σ_c is dominant in, σ_{tot}, $\sigma_s = 13$ Å, much larger than σ_s. This indicates that it is almost impossible for such σ_s to be the same from bottom to top interfaces, and it has to increase with film growth. In our analysis, we took into account the fact that the correlated roughness σ_s complied with the dynamic scaling law, the jth interface correlated roughness was expressed as $\sigma_{c,j} = (\sigma_{c,\min}^2 + [(N-j)/N]^{2\beta}(\sigma_{c,\max}^2 - \sigma_{c,\min}^2))^{1/2}$, and $\sigma_{c,\min}$ was set close to σ_s in simulation process. The best fits for off-specular intensity and rocking curves are shown by solid lines in Figs. 1 and 2, the corresponding parameters were listed in Table I. All experimental data were treated as one dataset, which means all data were fit simultaneously. This way could minimize possible errors due to interplay between parameters in the analysis, and all parameters given in Table I are used to explain all scans.

The fact that $\xi_{\|}$ increased from 500 to 2400 Å and σ_s increased from 6 to 13 Å indicates that the interfaces are locally flatter as the film grows. According to the relation $\sigma_{\text{tot}} = (\sigma_c^2 + \sigma_d^2)^{1/2}$, we obtained the interdiffusion width σ_d as 3 Å. Compared with σ_{tot}, the interdiffusion width is small, which means that the interdiffusion effect is not dominating in the layer-by-layer self-assembled method for the conjugated polymer multilayer. The vertical correlation length $\xi_{\perp}$ was obtained as 400 Å.

In conclusion, we have used x-ray reflectivity and off-specular diffuse scattering to study the interfacial structure of a self-assembled heterostructure through alternate deposition of conjugated and nonconjugated polymers. The Paratt formalism and DWBA theory were used to analyze specular

reflectivity and nonspecular scattering intensities. All data were fitted simultaneously to minimize possible error, and the obtained parameters could explain both specular and nonspecular scans. The fitting results indicate that the lateral correlation length and correlated roughness both obey the dynamical power law, and their values were given at each interface. It also shows that the interfaces of our sample become locally flatter with film growth.

This work was supported by a grant from the Ministry of Education, China. J.W. acknowledges the Korea-China Young Scientists Exchange Program for financial support.

*Present address: Baker Lab., Department of Chemistry and Chemical Biology, Cornell University, Ithaca, NY 14853. Email address: jw322@cornell.edu

[1] G. Decher, B. Lehr, K. Lowack, Y. Lvov, and J. Schmitt, Biosens. Bioelectron. **9**, 1 (1994).
[2] J. Tian, C. C. Wu, M. E. Thompson, J. C. Sturm, R. A. Register, M. J. Marsella, and T. M. Swager, Adv. Mater. **4**, 395 (1995).
[3] H. Hong, D. Davidov, H. Chayer, E. Z. Faraggi, M. Tarabia, Y. Avny, R. Neumann, and S. Klrestein, Supermol. Sci. **4**, 67 (1997).
[4] F. F. So and S. R. Forrest, Phys. Rev. Lett. **66**, 2649 (1991).
[5] Y. Ohmori, A. Fuji, M. Uchida, C. Morishima, and K. Yoshino, Appl. Phys. Lett. **62**, 3250 (1993).
[6] M. Tarabla, H. Hong, D. Davidov, S. Kirstein, R. Steitz, R. Neumann, and Y. Avny, J. Appl. Phys. **83**, 725 (1998).
[7] D. G. Stearns, J. Appl. Phys. **71**, 4286 (1992).
[8] D. E. Savage, Y. H. Phang, J. J. Rownd, J. F. MacKay, and M. G. Lagally, J. Appl. Phys. **74**, 6158 (1993).
[9] A. P. Payne and B. M. Clemens, Phys. Rev. B **47**, 2289 (1993).
[10] S. K. Sinha, M. K. Sanyal, S. K. Satija, C. F. Majkrzak, D. A. Neumann, H. Homma, S. Szpala, A. Gibaud, and H. Morkoc, Physica B **198**, 72 (1994).
[11] D. J. G. Boer, Phys. Rev. B **49**, 5817 (1994).
[12] R. Paniago, R. Forrest, P. C. Chow, S. C. Moss, S. S. P. Parkin, and D. Cookson, Phys. Rev. B **56**, 13 442 (1997).
[13] C. Thompson, G. Palasantzas, Y. P. Feng, S. K. Sinha, and J. Krim, Phys. Rev. B **49**, 4902 (1994).
[14] R. Schlatmann, J. D. Shindler, and J. Verhoeven, Phys. Rev. B **51**, 5345 (1995).
[15] J. P. Schlomka, M. Tolan, L. Schwalowsky, O. H. Seeck, J. Stettner, and W. Press, Phys. Rev. B **51**, 2311 (1995).
[16] J. Wang, D. R. Lee, C. Park, Y. H. Jeong, K. B. Lee, Y. J. Park, S. B. Youn, J. C. Park, H. M. Choi, and Y. J. Huh, Appl. Phys. Lett. **75**, 3775 (1999).
[17] Q. Shen, C. C. Umbach, B. Weselak, and J. M. Blakely, Phys. Rev. B **53**, R4237 (1996).
[18] L. G. Parratt, Phys. Rev. **95**, 359 (1954).
[19] M. Born and E. Wolf, *Principles of Optics*, 2nd ed. (Pergamon, Oxford, 1964).
[20] L. Nevot and P. Croce, Rev. Phys. Appl. **15**, 761 (1980).
[21] V. Holy and T. Baumbach, Phys. Rev. B **49**, 10 668 (1994).
[22] J. Stettner, L. Schwalowsky, O. H. Seeck, M. Tolan, W. Press, C. Schwarz, and H. v. Kanel, Phys. Rev. B **53**, 1398 (1996).
[23] S. K. Sinha, E. B. Sirota, S. Garoff, and H. B. Stanley, Phys. Rev. B **38**, 2297 (1988).
[24] V. Holy, J. Kubena, I. Ohlidal, K. Lischka, and W. Plotz, Phys. Rev. B **47**, 15 896 (1993).
[25] D. R. Lee, Y. J. Park, D. Kim, Y. H. Jeong, and K. B. Lee, Phys. Rev. B **57**, 8786 (1998).
[26] Y. Yoneda, Phys. Rev. **131**, 2010 (1963).
[27] F. Family, Physica A **168**, 561 (1990).
[28] A. L. Barabasi and H. E. Stanley, *Fractal Concepts in Surface Growth* (Cambridge University, Cambridge, 1995).
[29] M. Kardar, G. Parisi, and Y. Zhang, Phys. Rev. Lett. **56**, 889 (1986).
[30] G. W. Gollins, S. A. Letts, E. M. Fearon, R. L. McEachern, and T. P. Bernat, Phys. Rev. Lett. **73**, 708 (1994).
[31] J. Wang, G. Li, P. Yang, M. Q. Cui, X. M. Jiang, B. Dong, and H. Liu, Europhys. Lett. **42**, 283 (1998).